Ixazomib Induces Apoptosis and Suppresses Proliferation in Esophageal Squamous Cell Carcinoma through Activation of the c-Myc/NOXA Pathway[S]

Tianxiao Wang,[1] Pengying Zhang,[1] Lu Chen, Huijie Qi, Haifei Chen, Yongjun Zhu, Liudi Zhang, Mingkang Zhong, Xiaojin Shi, and Qunyi Li

Departments of Pharmacy (T.W., P.Z., L.C., H.Q., H.C., L.Z., M.Z., X.S., Q.L.) and Cardio-Thoracic Surgery (Y.Z.), Huashan Hospital, Fudan University, Shanghai, China

Received July 14, 2021; accepted October 18, 2021

ABSTRACT

Esophageal squamous cell carcinoma (ESCC) is one of the major subtypes of esophageal cancer. More than half of the patients with ESCC in the world are in China, and the 5-year survival rate is less than 10%. As a new oral proteasome inhibitor, ixazomib has shown strong therapeutic effect in many solid tumors. In this study, we aimed to investigate the effects of ixazomib on the proliferation inhibition and apoptosis of ESCC cells. We used four human ESCC cell lines, cell viability assay, cell cycle and apoptosis assay, reverse-transcription polymerase chain reaction (RT-PCR), Western blot, immunohistochemistry, and ESCC xenografts model to clarify the roles of the therapeutic effect and mechanism of ixazomib in ESCC. Ixazomib significantly inhibited the proliferation and induced apoptosis in ESCC cells. RT-PCR results showed that the expressions of endoplasmic reticulum stress–related gene phorbol-12-myristate-13-acetate–induced protein 1 (NOXA) and MYC proto-oncogene (c-Myc) significantly increase after treatment with ixazomib in ESCC cells. When we knocked down the NOXA and c-Myc by small interfering RNA, the therapeutic effect of ixazomib markedly decreased, which confirmed that c-Myc/NOXA pathway played a key role in the treatment of ESCC with ixazomib. In vivo, the xenograft ESCC model mice were given 10 mg/kg of ixazomib every other day for 30 days. The results showed that the tumor size in the treatment group was significantly smaller than the control group. These results suggested that ixazomib is known to suppress proliferation and induce apoptosis in ESCC cell lines, and this effect was likely mediated by increased activation of the c-Myc/NOXA signaling pathways.

SIGNIFICANCE STATEMENT

Esophageal squamous cell carcinoma (ESCC) is the common worldwide malignant tumor, but conventional chemotherapeutics suffer from a number of limitations. In this study, the results suggested that ixazomib suppresses proliferation and induces apoptosis in ESCC cell lines. Therefore, ixazomib may be a potential new strategy for ESCC therapy.

Introduction

Currently, esophageal cancer is the seventh most common worldwide malignant tumor. More than 456,000 new cases of esophageal cancer and 300,000 deaths were recorded globally in 2018, which accounted for 3.2% and 5.3% of all cancers, respectively (Bray et al., 2018). According to histopathological classification, esophageal cancer is composed of two main histologic subtypes, esophageal squamous cell carcinoma (ESCC) and esophageal adenocarcinoma.

East Asia is a region with a high incidence of esophageal cancer, and China accounts for approximately half of the world's esophageal cancer cases (Ferlay et al., 2010). Notably, more than 90% of patients are diagnosed with ESCC in China (Zhao et al., 2012; Liang et al., 2017). The major treatment of patients with ESCC is surgical resection, and the prognosis is favorable in the early stages, but the early symptoms of ESCC are more hidden, invasive, and aggressive because most diagnosed patients with ESCC are in moderate and advanced stages (Mariette et al., 2007). Therefore, for these patients, chemotherapy helps to reduce the primary tumor bulk, increase the possibility of radical resection, and treat micrometastatic disease and prolong the survival period of patients (Lordick et al., 2016). These chemotherapeutic drugs include combinations of platinum-based drugs, 5-fluorouracil, paclitaxel, and doxorubicin.

ABBREVIATIONS: Bcl-2, BCL2 apoptosis regulator; CCK-8, Cell Counting Kit-8; CI, combination index; c-Myc, MYC proto-oncogene; ERS, endoplasmic reticulum stress; ESCC, esophageal squamous cell carcinoma; G, growth; HECC, human esophageal epithelial cell; M, mitosis; NOXA, phorbol-12-myristate-13-acetate–induced protein 1; PI, propidium iodide; RT-PCR, reverse-transcription polymerase chain reaction; sic-Myc, c-Myc siRNA; siNOXA, NOXA siRNA; siRNA, small interfering RNA; TUNEL, terminal deoxynucleotidyl transferase–mediated digoxigenin-deoxyuridine nick-end labeling.

However, conventional chemotherapeutics is often seriously hindered by a number of limitations, including high-systemic toxicity, chemoresistance, and short in vivo circulation half-life.

Currently, targeted therapy was recognized as a promising strategy for cancer treatment because of its high specificity and minimal side effects. The ubiquitin-proteasome system plays a critical role in regulating 80%–90% of protein degradation and turnover as well as regulation of multiple cellular events, including the cell cycle, signal transduction, response to oxidative stress, cell proliferation, and apoptosis (Ciechanover, 1994; Hochstrasser, 1995; Jana, 2012). As the critical endpoint for the ubiquitin-proteasome system, the 26S proteasome is the chief proteolytic effector responsible for recognizing and degrading the ubiquitylated protein, which consists of a core particle 20S proteasome and two 19S regulatory particles (Bard et al., 2018). In the past decade, proteasome has gained increasing attention as a target for cancer treatment. Among them, the proteasome inhibitor (e.g., bortezomib and carfilzomib) has been confirmed to show excellent therapeutic effects in the treatment of multiple myeloma and other tumors (Johnson, 2015; Manasanch and Orlowski, 2017).

Ixazomib, an oral 20S subunit-selective inhibitor being developed to be used for treatment of a broad range of human malignant tumors. Compared with bortezomib, ixazomib has a shorter proteasome dissociation half-life, which has a critical role in improving the distribution of the drug in solid tumor tissues (Kupperman et al., 2010). Currently, ixazomib was approved for treatment of patients with multiple myeloma, in combination with lenalidomide and dexamethasone, by the US Food and Drug Administration (Shirley, 2016). Besides hematologic neoplasms, a series of studies have suggested that ixazomib also has therapeutic anticancer functions in solid tumors, including colorectal cancer, bladder cancer, osteosarcoma, and breast cancer (Kupperman et al., 2010; Sato et al., 2017; Yue and Sun, 2019; Harris et al., 2020). However, the detailed mechanisms underlying ixazomib-induced cancer cell death remain unclear.

In recent years, the endoplasmic reticulum stress (ERS) pathway has been discovered to regulate cellular processes, including protein folding, sorting, and secretion and play a crucial role in the process of apoptosis (Oakes and Papa, 2015; Minchenko et al., 2016). Early ERS is a response promoting survival, whereas the unfolded protein response reduces the accumulation of unfolded protein and restores the function to the endoplasmic reticulum (Oakes and Papa, 2015). However, when the unfolded protein response is not sufficient to protect cell survival, the endoplasmic reticulum will act as the trigger point of apoptosis signals to induce apoptosis and promote the expression of apoptosis-inducing factors, such as the BCL2 apoptosis regulator (Bcl-2) homology 3–only proapoptotic protein phorbol-12-myristate-13-acetate–induced protein 1 (NOXA), which is a key mediator for ERS-induced apoptosis (Kelly et al., 2012; Cano-Gonzalez et al., 2018). Proteasome inhibitor MG-132 was found to induce apoptosis via activation of NOXA signaling pathways in hepatic stellate and chronic lymphocytic leukemia cell lines (Baou et al., 2010; Sosa Seda et al., 2010). Furthermore, many studies have found evidence of sustained and high-level activation of ERS in esophagus cancer cells (Rosekrans et al., 2015; Hu et al., 2019). These studies suggest that ixazomib could potentially be used to induce ESCC cell apoptosis via ERS-mediated NOXA induction.

In the present study, we evaluated the preclinical efficacy of ixazomib in ESCC cell lines and animal xenograft models by a series of in vitro and in vivo experiments. Our results demonstrate that that ixazomib is strongly apoptotic and blocks ESCC cell growth and survival. We further show that ixazomib exerts its proapoptotic action via a mechanism involving the activation of the NOXA–MYC proto-oncogene (c-Myc) pathway. These results indicate that ixazomib may be an additional useful strategy to improve the treatment outcome for patients with ESCC.

Materials and Methods

Cell Culture. The human esophageal squamous carcinoma cell lines KYSE 150, KYSE 510, KYSE520, TE1 and human esophageal epithelial cell (HECC) lines were purchased from American Type Culture Collection (Manassas, VA). KYSE 150, KYSE520, and TE1 were cultured in RPMI 1640 medium (HyClone, Logan, UT). KYSE 510 were cultured in 50% F12 medium (Hyclone) and 50% RPMI 1640 mixed medium. HECC cultured in high glucose minimum essential medium (Hyclone). Both media were supplemented with 10% FBS (Yeasen Biologic Teachnology Co., Ltd, Shanghai, China) and 100 U/ml penicillin/streptomycin (Wisent, Saint-Bruno, QC) at 37°C in a humidified incubator with 5% CO_2 and 95% air.

Reagents. Ixazomib purchased from Med Chem Express (HY-10453, Monmouth Junction, NJ) were dissolved in DMSO. These reagents were stored at −20°C until use.

Cell Viability Assay. The cell viability assay was performed using the Cell Counting Kit-8 (CCK-8) (Proteintech Group, Inc, Rosemont, IL). Briefly, the ESCC cells were seeded into 96-well plates at 6×10^3 cells/well and incubated under standard culture conditions for 24 hours, and then the cells were treated with gradient concentrations of ixazomib for 24–72 hours. After treatment, 10 μl of CCK-8 solution was added into each well of the 96-well plate and incubated for 1 hour at 37°C. The optical density values were detected at 450 nm using a microplate reader (Biotek, Winooski, VT). Each experiment was independently repeated three times with five replicates.

Colony Formation Assay. For colony formation assay, KYSE150 and KYSE510 cells were plated in six-well plates (1×10^3 cells/well) and cultured under standard culture conditions overnight. Then, the medium was replaced with gradient concentrations of ixazomib and vehicle for 2 weeks until the colonies were visible in the culture plate. The supernatants were discarded and washed twice with PBS, 4% paraformaldehyde used to fix the colonies, and stained with 0.1% crystal violet solution for 30 minutes. Finally, the excess staining solution was washed away with distilled water and photographed on a microscope using Image J software to calculate the number of clones.

Cell Cycle Analysis. For cell cycle analysis, we used the Cell Cycle Kit (Beyotime, Shanghai, China). KYSE150 and KYSE510 cells were treated with vehicle (0.1% DMSO) or ixazomib (0.25, 0.5, and 1 μM) for 24 hours. Then, these cells were washed three times with PBS (0.1M, pH 7.4) and fixed in 70% ethanol solution at −20°C overnight. The fixed cells were washed with cold PBS to remove excess ethanol solution and stained with propidium iodide (PI) staining buffer. Samples were incubated at 37°C for half an hour and using BD Accuri C6 (BD Biosciences, Franklin Lakes, NJ) for assay. The experiments were repeated three times, and data were analyzed with ModFit LT software (Verity Software House, Topsham, ME).

Cell Apoptosis and Caspase-3 Activity Determination. For simultaneous measurement of cell apoptosis, we used the Annexin V-FITC/PI apoptosis kit (Beyotime) according to the manufacturer's instructions. KYSE150 and KYSE510 cells were treated with vehicle (0.1% DMSO) or ixazomib (0.25, 0.5, and 1 μM) for 24 hours. Then, the cells were harvested and washed twice with cold PBS, and Annexin binding buffer (500 μl) was added to each sample. Thereafter, cells were stained by Annexin V-FITC and PI solution in the dark for 15 minutes. The stained cells were analyzed by flow cytometry (NovoCyte; ACEA Biosciences, San Diego, CA) at the fluorescence emission of 530 nm.

Because the activation of caspase-3 represents an essential step in the apoptotic process, the GreenNuc Caspase-3 Assay Kit (Beyotime) was used to count caspase-3 activity in cells according to the manufacturer's introductions. Esophageal cancer cells were treated with vehicle (0.1% DMSO) or ixazomib (0.5 and 1 μM) for 24 hours, and caspase-3 positive cells were observed and counted by fluorescence microscope.

Western Blot Analysis. Western blotting was done as described previously (Zhang et al., 2019). Bcl-2, NOXA, c-Myc, cleaved caspase-8, and cleaved caspase-9 (Cell Signaling Technology, Danvers, MA) were used as primary antibodies. These primary antibodies were followed by appropriate secondary antibodies conjugated to horseradish peroxidase. Antibody-protein complexes were detected using enhanced chemiluminescence immunoblotting detection reagent. The signals were analyzed using a LAS-3000 image analyzer and MultiGauge software (Fujifilm Corporation, Tokyo, Japan). Densitometric analysis of Western blot results was performed with ImageJ software.

Quantitative Real-Time Polymerase Chain Reaction. KYSE-150 cells were treated with DMSO (0.1%) or ixazomib (10 μM) for 24 hours. Total RNA was isolated using the Trizol reagent and Ultrapure RNA kit (CW Biotech, Beijing, China) according to the manufacturer's instructions. Two milligrams of total mRNA was reverse-transcribed with the Superscript reverse-transcription system (Takara, Dalian, Japan). Quantitative real-time reverse-transcription polymerase chain reaction (RT-PCR) was carried out on ABI 7500 Real-Time PCR system (Applied Biosystems, Foster City, CA) using SYBR Green PCR master mix reagents (Takara). Relative quantification of target gene mRNA level was calculated after normalization to glyceraldehyde-3-phosphate dehydrogenase mRNA using the method. The primer sequences were selected based on the published literature (Du et al., 2017).

Gene Silencing Using Small Interfering RNA. Kyse150 and Kyse510 cells were transfected using LipofectAMINE 2000 (Life Technologies, Carlsbad, CA) with small interfering RNA (siRNA) mixture targeting NOXA or c-Myc for 48 hours and further treated with ixazomib (1 μM) for another 48 hours. Then, cells were collected for cell viability assay. The siRNA [NOXA siRNA (siNOXA) and c-Myc siRNA (sic-Myc)] and control siRNA were purchase from HanBio Technology Co. Ltd. (HanBio, Shanghai, China).

The sequences of the siRNA are as follows: siNOXA#1: GUAAUU AUUGACACAUUUC, siNOXA#2: GGUGCACGUUUCAUCAAUUUG, sic-Myc#1: AACGUUAGCUUCACCAACA, and sic-Myc#2: CGAGCU AAAACGGAGCUUU.

Esophageal Squamous Carcinoma Xenografts. Human esophageal squamous carcinoma cell xenografts were generated by subcutaneously injecting 2×10^6 KYSE150 cells suspended with PBS/Matrigel into the right flank region of 6-week-old BALB/c nude mice (Zhang et al., 2016). Tumor growth was monitored once every 5 days after implantation. When subcutaneous tumors reached an average size of greater than 100 mm³, mice were intragastrically treated with ixazomib or vehicle (5% DMSO + 45% PEG300 + ddH$_2$O). During the study, mice were weighed every 10 days during and after the drug treatments. Tumor volumes were calculated using the formula V = length × width^2 × 0.5, where length and width represent the longer and shorter tumor diameters, respectively. All procedures were performed in accordance with approved protocols by the Fudan University Institutional Animal Care and Use Committee. Every effort was made to minimize potential distress, pain, or discomfort to the animals throughout all experiments.

Histopathology and Immunohistochemistry. Tumor tissues obtained from the mice bearing KYSE150 tumors were subjected to immunohistological analysis. Briefly, at the end of the treatment, mice were killed, and tumor tissues were obtained. Immunohistological detection of anti–c-Myc (#9402, Cell Signaling Technology) and NOXA (#14766, Cell Signaling Technology) were performed according to the manufacturer's instructions using paraffin-embedded sections
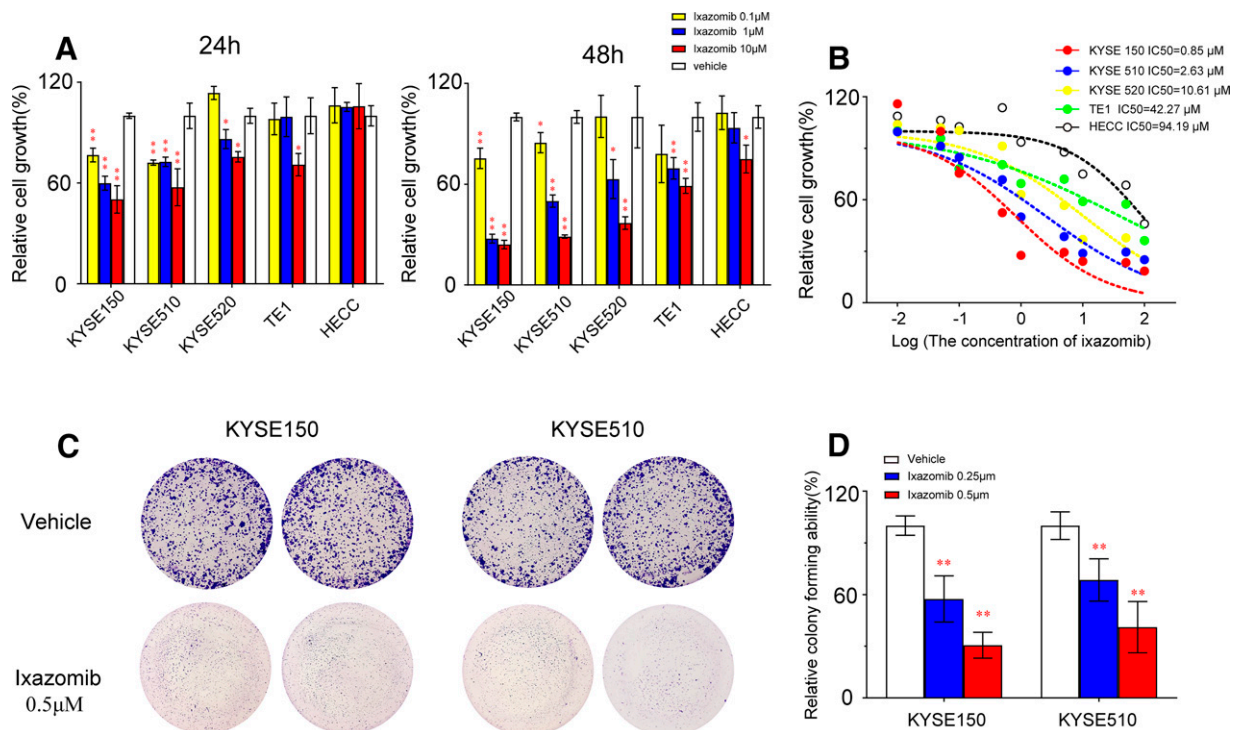

Fig. 1. Ixazomib inhibits growth and colony formation of esophageal squamous carcinoma cells. (A) Effect of ixazomib on the viability of breast cancer cells Kyse150, Kyse510, Kyse520, TE1, and HECC. Cells were treated with vehicle or ixazomib (0.1, 1, and 10 μM) for 24 and 48 hours, and the viability was detected with the CCK-8 kit. (B) ESCC cells were treated with various concentrations of ixazomib for 24 hours. Cell viability was determined by the CCK-8 assay. The IC$_{50}$ value of ixazomib in ESCC cell lines was then determined. (C and D) Efficacy of ixazomib on colony formation of ESCC cells. ESCC cells were treated with ixazomib (0.25 and 0.5 μM) for 7 days and then fixed, stained, and counted. Values are presented as mean ± S.D. ($n = 3$). *$P < 0.05$ or **$P < 0.01$ indicates significant differences from the vehicle group as assessed by a one-way ANOVA with a post hoc Dunnett's test.

of tumor. Apoptotic cells in the tumor tissue were detected by terminal deoxynucleotidyl transferase–mediated deoxyuridine nick-end labeling (TUNEL) staining using an apoptotic cell detection kit (Beyotime). Additionaly, the major organs were removed for histologic examination by H&E staining.

Statistical Analysis. GraphPad Prism 7.0 and SPSS 16.0 software were used for statistical evaluation. Group differences in vitro experiments were compared by performing a one-way ANOVA with Dunnett's post hoc test, and we used the Chou-Tallay isobologram by compusyn software to evaluate the synergistic effect of ixazomib combined with cisplatin and 5-fluorouracil. The animal experiments were compared using independent-samples Student t tests. Prior to analysis, all data underwent the Kolmogorov-Smirnov normality test and Levene's test;

results showed that all data from different groups of data satisfied the normality and homogeneity of variance. Data are expressed as mean ± S.D. $P < 0.05$ was considered statistically significant.

Results

Ixazomib Inhibited the Proliferation of Human Esophageal Squamous Carcinoma Cells. Ixazomib is an orally available proteasome inhibitor that potently, reversibly, and selectively targets the proteasome. Here, we aimed to evaluate its therapeutic potential toward esophageal squamous carcinoma. Cell viability assay and colony formation
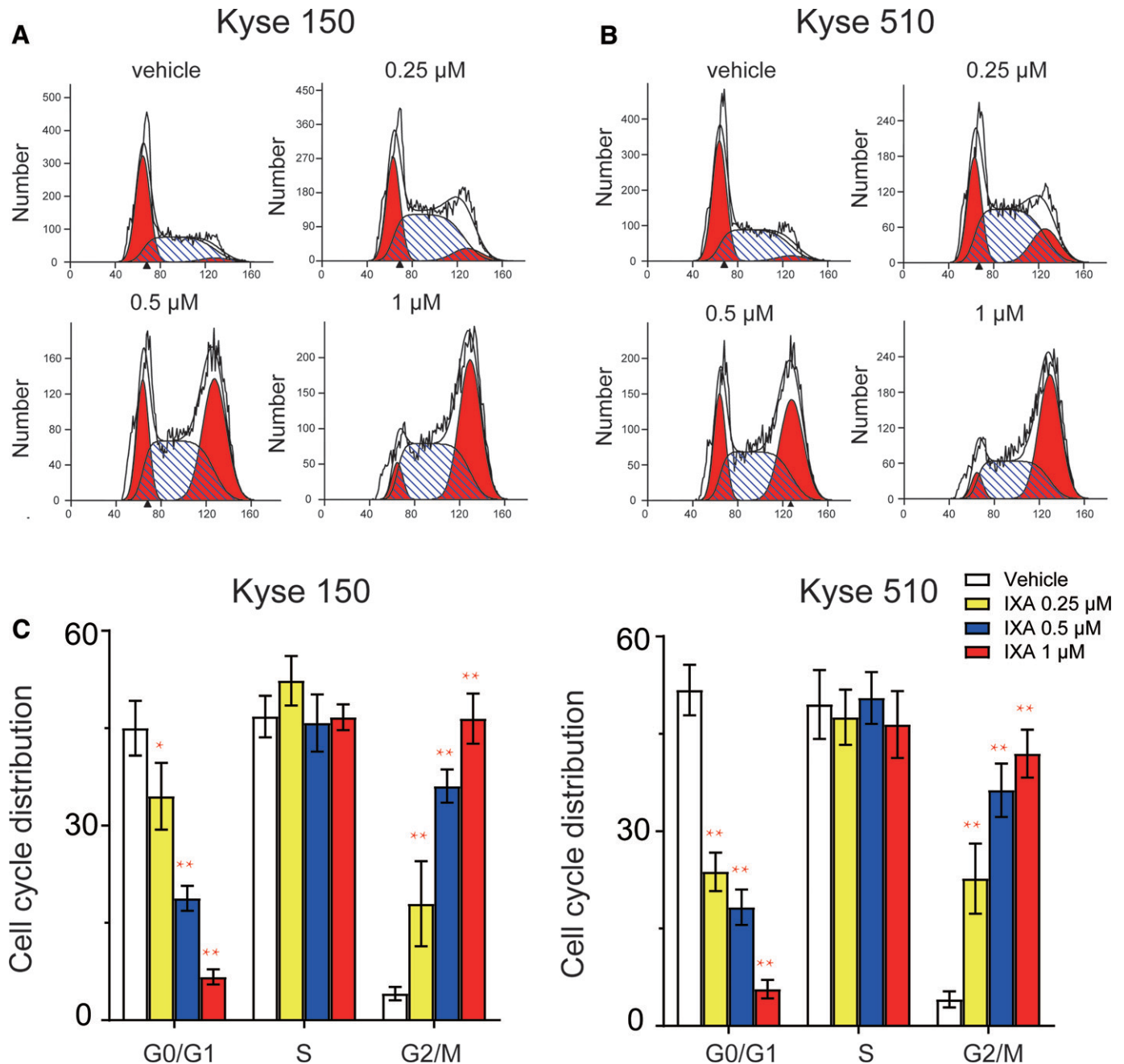

Fig. 2. Ixazomib triggers G2/M cell cycle arrest in esophageal cancer cells. (A and B) Ixazomib induced G2/M cell cycle arrest in Kyse150 and Kyse510 cells treated with ixazomib at different concentration for 24 hours, followed by PI staining and fluorescence-activated cell sorting (FACS) analysis for cell cycle profile. (C) Distribution was analyzed by Modift and GraphPad software (lower panel). Values are presented as mean ± S.D. (n = 5–6). *$P < 0.05$ or **$P < 0.01$ indicates significant differences from the vehicle group as assessed by a one-way ANOVA with a post hoc Dunnett's test. S, synthesis.
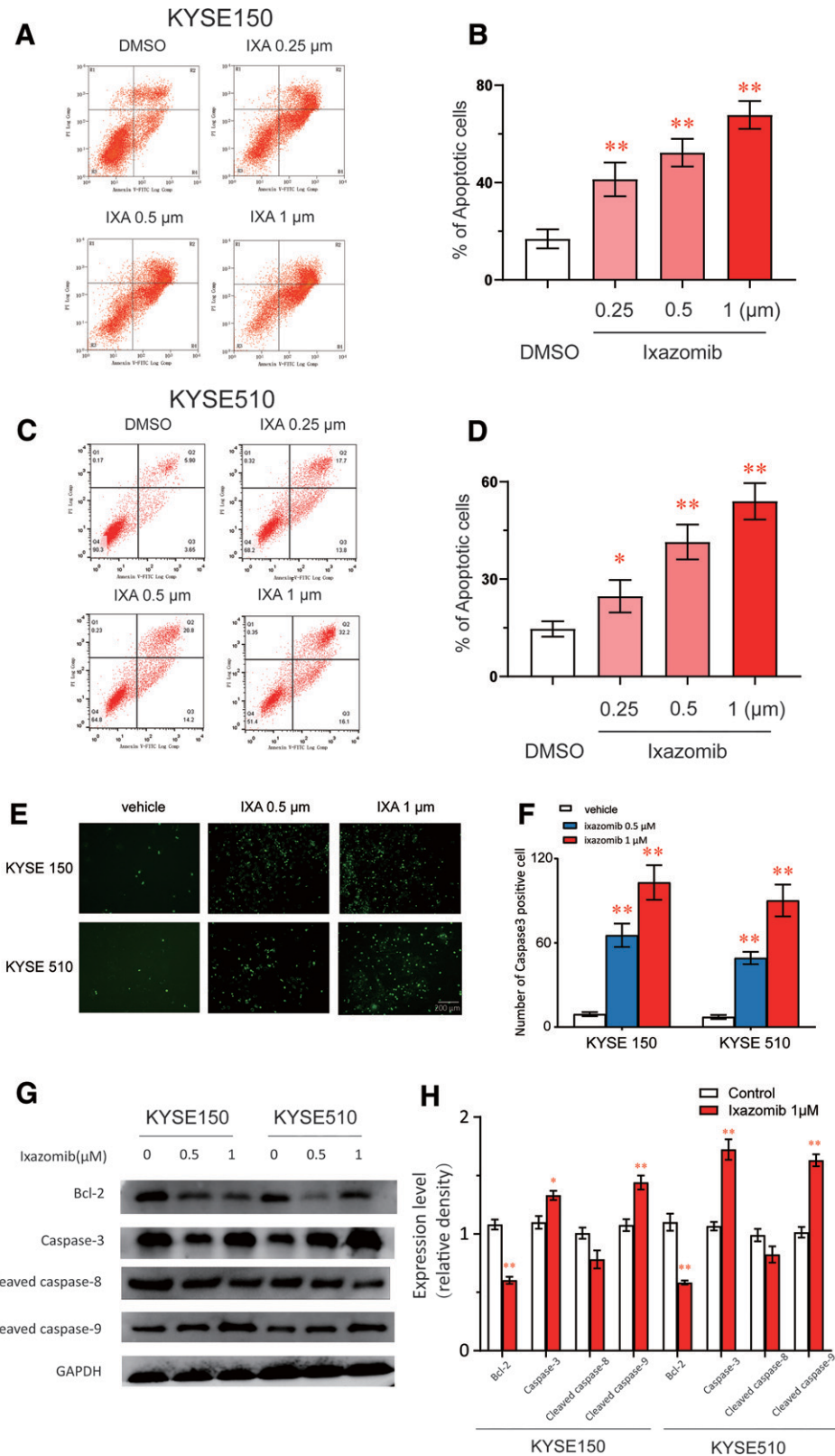
Fig. 3. Ixazomib induces apoptosis in ESCC. Kyse150 and Kyse510 cells were treated with ixazomib for 48 hours. (A–D) Apoptosis was determined by fluorescence-activated cell sorting (FACS) analysis using Annexin V-FITC/PI double-staining kit, and Annexin V–positive cell populations were defined as apoptosis. (E and F) The GreenNuc Caspase-3 Assay Kit was used to observe the expression of caspase-3 in live esophageal cancer cells after treatment with ixazomib. (G and H) Treatment with ixazomib increased the expression of caspase-3, cleaved caspase-9, and decreased the expression of Bcl-2. ESCC cells were treated with ixazomib for 48 hours, and cell lysates were assessed by Western blot. Glyceraldehyde-3-phosphate dehydrogenase (GAPDH) was used as loading control. Values are presented as mean ± S.D. (n = 5–6). *$P < 0.05$ or **$P < 0.01$ indicates significant differences from the vehicle group as assessed by a one-way ANOVA with a post hoc Dunnett's test. IXA, ixazomib.

assay were used to explore the anticancer effect of ixazomib in four commonly used ESCC cell lines. Results showed that ixazomib displays excellent antiproliferation activity as measured by the CCK-8 assay in ESCC cell lines. Treatment with 1 μM ixazomib inhibited cell viability by 40.3%, 27.4%, and 13.5% at 24 hours and 72.5%, 50.1%, and 37.4% at 48 hours for KYSE150, KYSE510, and KYSE520, respectively (P < 0.05 for all), but the inhibition of cell viability was slightly weaker in TE1 cell lines than in other cell lines (Fig. 1A). And with an IC$_{50}$ value at 0.85, 2.63, 10.61, and 42.27 μM for KYSE150, KYSE510, KYSE520, and TE1 cell line, respectively (Fig. 1B). We also found that ixazomib had no effect on proliferation in the HECC line. The measurement of cell viability demonstrated that Kyse150 and Kyse510 cells were more sensitive to ixazomib treatment; therefore, we selected these ESCC cell lines in the after study.

When evaluated by the colony formation assay, high-dose ixazomib (0.5 μM) significantly reduces in the number of colonies by 58.9% and 69.4% for KYSE150 and KYSE510, respectively (P < 0.01 for both) (Fig. 1, C and D). All these findings demonstrate that ixazomib has anticancer activity toward ESCC.

Ixazomib Induced G2/M Cell Cycle Arrest. To understand the underlying mechanisms of antiproliferative activity of ixazomib, we first examined the effect of ixazomib-treated ESCC cells. The Kyse150 and Kyse510 cells were treated with a gradient concentration of 0.25, 0.5, and 1 μM ixazomib for 24 hours. The results show that a dose-dependent increase of cells in the growth (G) 2/mitosis (M) phase indicated the ixazomib induction of a G2/M phase arrest (Fig. 2, A and B). The results revealed that ixazomib treatment increased the expression of G2/M phase–related proteins p21 (Fig. 2C). These results suggest that ixazomib has been found to induce cell cycle arrest in G2/M phase in ESCC cells.

Ixazomib Promotes Apoptosis in ESCC Cells. ESCC cells treated with ixazomib shrank, and turnaround was observed microscopically after 48 hours, which suggested that ixazomib treatment could trigger apoptosis. Therefore, we used the Annexin V-FITC/PI assay to confirm this speculation. In the apoptotic assays, Kyse150 and Kyse510 cells treated with ixazomib at 0.25–1 μM increased the Annexin V–positive cell populations in a dose-dependent manner (Fig. 3, A–D). Additionally, we used the GreenNuc Caspase-3 Assay Kit to observe the expression of caspase-3 in live esophageal cancer
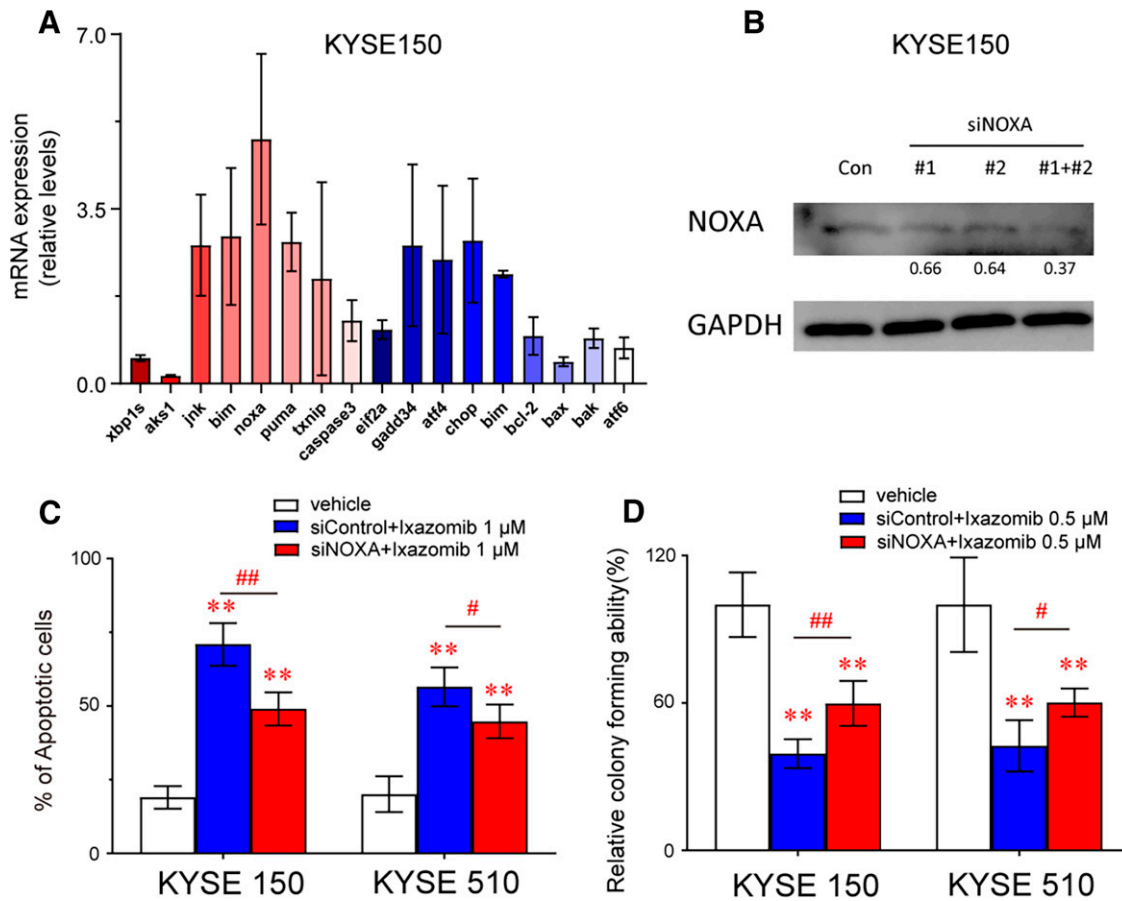

Fig. 4. NOXA participates in ixazomib-induced proliferation inhibition in ESCC cells. (A) Kyse150 cell treated with or without 1μM ixazomib for 48 hours. The expression of ERS-related gene was examined by RT-PCR. (B) Western blots assay was used to evaluate the knockdown effect of single siRNA and pooled siRNA on NOXA protein. (C and D) After being transfected with the NOXA siRNA for 48 hours, Kyse150 and Kyse510 cells were further treated with ixazomib (1 μmol) for 48 hours, and the cell apoptosis and colony formation were examined. Values are presented as mean ± S.D. (n = 4–5). *P < 0.05 or **P < 0.01 indicates significant differences from the vehicle group, and ##P < 0.01 indicates significant differences from the siRNA control (siControl) group as assessed by a one-way ANOVA with a post hoc Dunnett's test. ask1, ABA-responsive kinase substrate 1; atf4/6, activating transcription factor 4/6; bak, BCL2 antagonist/killer 1; bax, BCL2 associated X; bcl-2, BCL2 apoptosis regulator; bim, BCL2 like 11; chop, DNA damage inducible transcript 3; eif2a, eukaryotic translation initiation factor 2A; gadd34, protein phosphatase 1 regulatory subunit 15A; jnk, mitogen-activated protein kinase 8; puma, BCL2 binding component 3; txnip, thioredoxin interacting protein; xbp1s, X-box binding protein 1.

cells after treatment with ixazomib. The results showed that the number of caspase-3–positive cells was significantly increased in the ixazomib (0.5 and 1μM) treatment group compared with the control group in kyse 150 and kyse 510 cells (Fig. 3, E and F). Additionally, ixazomib treatment and the activation of caspase-3, cleaved caspase-9, and inhibition of Bcl-2 was confirmed by Western blot analysis in ESCC cells (Fig. 3, G and H), which suggested that ixazomib-induced apoptosis was involved in mitochondrial/intrinsic apoptosis pathway. These results confirmed that ixazomib could trigger apoptosis in ESCC cells.

c-Myc/NOXA Pathway Participates in Ixazomib-Induced Proliferation Inhibition in ESCC Cells. As in previous studies, the proteasome inhibitors increased the accumulation of polyubiquitinated proteins and triggered the endoplasmic reticulum stress–induced apoptosis in several cancer cells (Fribley et al., 2004; Mozos et al., 2011; Niewerth et al., 2015). To assess the role of the ixazomib in apoptosis by endoplasmic reticulum stress in ESCC cells, we determined by RT-PCR the expression levels of endoplasmic reticulum stress–related genes in Kyse150 cells treated with ixazomib. Results of these experiments showed a significant increase in the mRNA expression levels of endoplasmic reticulum stress–related genes in response to ixazomib. The increase in NOXA expression was the most prominent compared with other ERS-related genes (Fig. 4A). We knocked down the NOXA by siRNA, the results show that siNOXA significantly decreased the expression level of NOXA protein in ESCC cells (Fig. 4B), and silencing NOXA rescued ixazomib-induced apoptosis, proliferation inhibition (Fig. 4, C and D), and cell viability inhibition (Supplemental Fig. 1, A and C) in ESCC cells.

Several studies have evidenced that c-Myc was a prime transcription factor to transactivate NOXA (Nikiforov et al., 2007; Knorr et al., 2015). We determined the protein levels of NOXA and c-Myc in both Kyse150 and Kyse510 cell lines in response to ixazomib. As shown in Fig. 5A, ESCC cells expressed undetectable NOXA protein levels, which were clearly upregulated after ixazomib treatment. Furthermore, the c-Myc protein expression followed a trend similar to that observed for NOXA protein expression. We knocked down the c-Myc by siRNA, and the expression of NOXA significantly decreased in Kyse150 under ixazomib treatment or basic state, which suggested that c-Myc plays an important role in the activation of NOXA by ixazomib (Fig. 5C). Additionally, the same phenomenon can be found that reduced c-Myc function and rescued ixazomib-induced apoptosis, proliferation inhibition (Fig. 5, D and E), and cell viability inhibition (Supplemental Fig. 1, B and D) in ESCC cells. These observations indicated that c-Myc/NOXA signaling pathways play a major role in ixazomib-induced proliferation inhibition in ESCC cells.

Cell Viability Inhibition Effect of Combination Treatments of Ixazomib and Chemotherapy Agents. Next, we assessed whether the combination of ixazomib and commonly used chemotherapy agents (cisplatin and 5-fluorouracil) exhibited additive or synergistic cell viability inhibition of ESCC cells. We applied a universal reference experimental scheme (Chou–Talalay isobologram analysis) for evaluating the effects of possible synergistic interaction (Ooko et al., 2017). The ESCC cell lines were treated with varying concentrations of ixazomib at indicated concentrations of cisplatin and fluorouracil for 24 hours. A combination index (CI) less than 1 indicates the drug combination has synergism. The results showed that the combination of low concentrations of
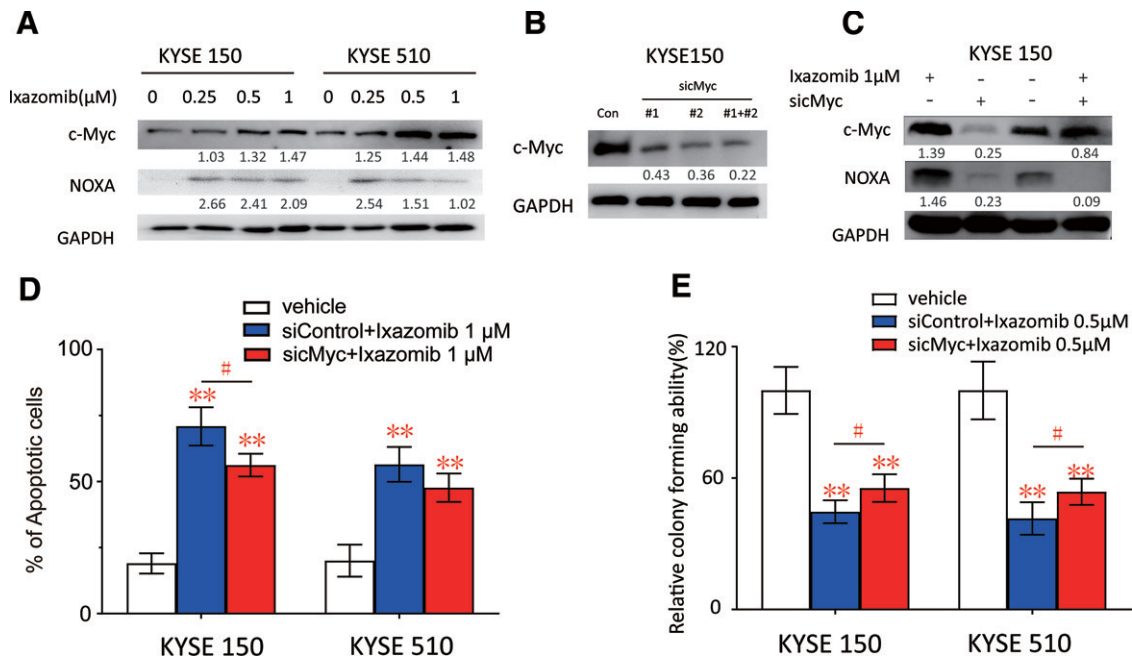
Fig. 5. c-Myc/NOXA pathway plays an important role in ixazomib-induced proliferation inhibition in ESCC cells. (A) Kyse150 and Kyse 510 were treated with or without 1 μM ixazomib for 48 hours. Cell lysate was prepared, and c-Myc and NOXA protein level was determined by Western blotting analysis. (B) Western blots assay was used to evaluate the knockdown effect of single siRNA and pooled siRNA on c-Myc protein. (C) The protein expression of NOXA in Kyse150 after knockdown of c-Myc. (D and E) After being transfected with the c-Myc siRNA for 48 hours, Kyse150 and Kyse510 cells were further treated with ixazomib (1 μmol) for 48 hours, and the cell apoptosis and colony formation were examined. Values are presented as mean ± S.D. (n = 4–5). *P < 0.05 or **P < 0.01 indicates significant differences from the vehicle group, ##P < 0.01 indicates significant differences from the siRNA control (siControl) group as assessed by a one-way ANOVA with a post hoc Dunnett's test.
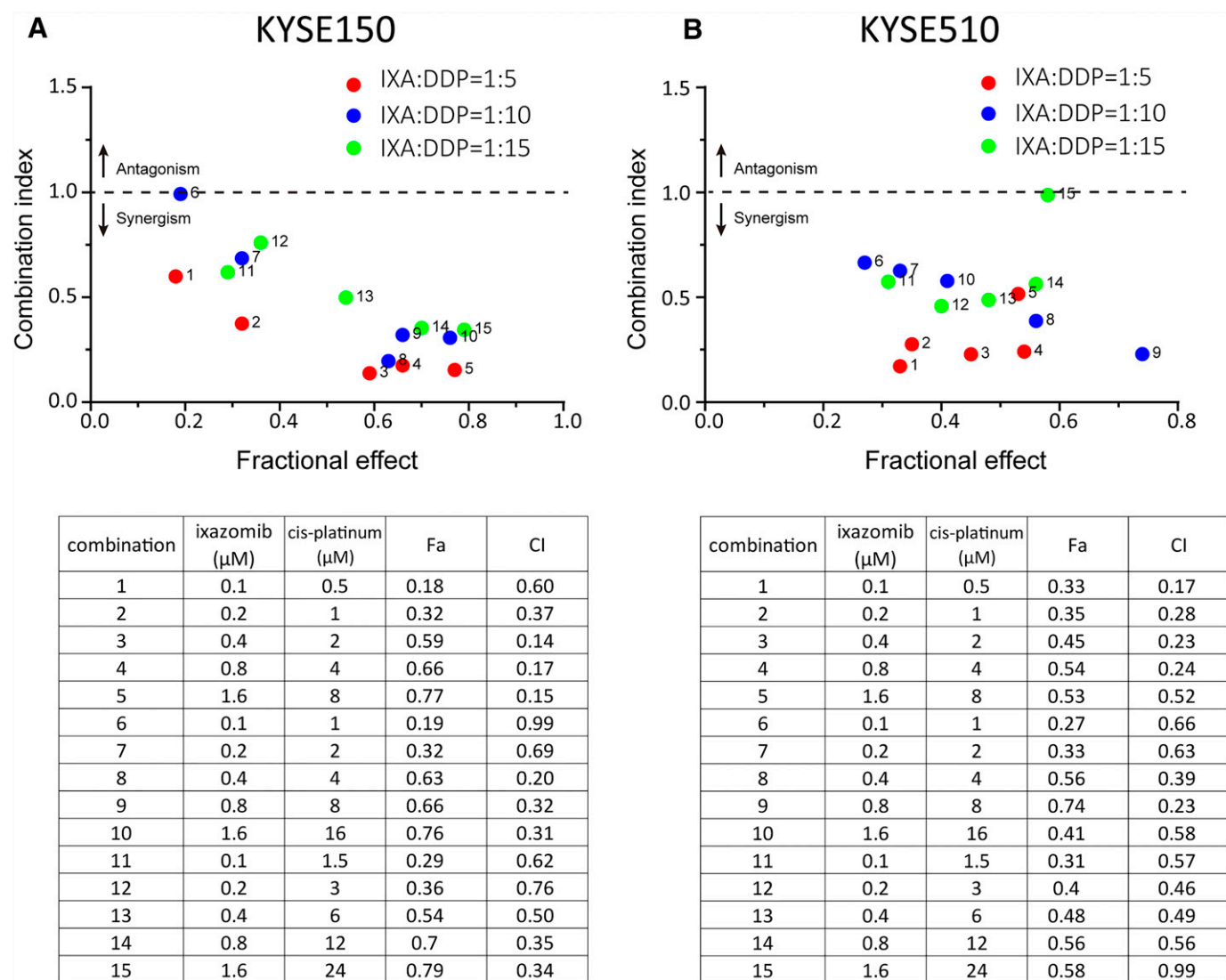
Fig. 6. Combination of low doses of ixazomib and cisplatin triggers synergistic anti-ESCC activity. KYSE150 (A) and KYSE510 (B) cells were treated for 24 hours with indicated concentrations of ixazomib, cisplatin, or ixazomib plus cisplatin and then assessed for viability by CCK8 assays. Isobologram analysis shows the synergistic cytotoxic effect of ixazomib plus cisplatin. The graph (top) is derived from the values given in the table (bottom). Numbers 1–15 in the graph represent combinations shown in the table. CI < 1 indicates synergy. All experiments were carried out in triplicate, and the mean value is shown. Fa, fraction of cells showing decrease in viability with ixazomib plus cisplatin treatment. DDP, cisplatin; IXA, ixazomib.

KYSE150 table:

combination	ixazomib (μM)	cis-platinum (μM)	Fa	CI
1	0.1	0.5	0.18	0.60
2	0.2	1	0.32	0.37
3	0.4	2	0.59	0.14
4	0.8	4	0.66	0.17
5	1.6	8	0.77	0.15
6	0.1	1	0.19	0.99
7	0.2	2	0.32	0.69
8	0.4	4	0.63	0.20
9	0.8	8	0.66	0.32
10	1.6	16	0.76	0.31
11	0.1	1.5	0.29	0.62
12	0.2	3	0.36	0.76
13	0.4	6	0.54	0.50
14	0.8	12	0.7	0.35
15	1.6	24	0.79	0.34

KYSE510 table:

combination	ixazomib (μM)	cis-platinum (μM)	Fa	CI
1	0.1	0.5	0.33	0.17
2	0.2	1	0.35	0.28
3	0.4	2	0.45	0.23
4	0.8	4	0.54	0.24
5	1.6	8	0.53	0.52
6	0.1	1	0.27	0.66
7	0.2	2	0.33	0.63
8	0.4	4	0.56	0.39
9	0.8	8	0.74	0.23
10	1.6	16	0.41	0.58
11	0.1	1.5	0.31	0.57
12	0.2	3	0.4	0.46
13	0.4	6	0.48	0.49
14	0.8	12	0.56	0.56
15	1.6	24	0.58	0.99

ixazomib and cisplatin triggered synergistic anti-ESCC activity, with a CI < 1.0 (Fig. 6, A and B). However, we observed no similar synergistic effects between ixazomib and 5-fluorouracil in ESCC cells (Supplemental Fig. 2). This phenomenon suggests that the combination of ixazomib and cisplatin has therapeutic potential in the treatment of ESCC.

Ixazomib Inhibits the Growth of ESCC Tumors in Mice Xenograft Models. Based on the results of in vitro studies, we hypothesized that ixazomib might have an antitumor effect in vivo. To address this hypothesis, ESCC tumor xenografts were established in nude mice. Figure 7A shows that ixazomib had a strong inhibition on the growth of human ESCC xenografts. At the final measurement, the volumes of tumors from the mice treated with a ixazomib dose of 10 mg/kg every other day were 745 mm^3, whereas the size of the tumors in control mice already reached 1340 mm^3. The tumor growth was inhibited by 44.4% after treatment with ixazomib

(Fig. 7F). Then, the tumor specimens from mouse xenografts were subjected to immunohistochemical staining for NOXA and c-Myc expression. The results show that elevated NOXA expression was accompanied by an increase in c-Myc expression level in the tumor tissue of the ixazomib-treated group compared with that in the vehicle-treated control (Fig. 7B). Additionally, 4′,6-diamidino-2-phenylindole and TUNEL staining results confirmed that compared with the control group, the apoptosis rate was markedly enhanced in the ixazomib-treated group. To observe the delayed organ toxicity in the mice within a certain treatment period, major organs including heart, liver, kidney and spleen from experimental mice administered with free ixazomib and ixazomib treatment were sectioned and stained with H&E. No obvious histopathological change was observed in heart, lung or spleen of ixazomib-treated mice, as shown in Fig. 7D. No significant drug-related effects on body weight or any other signs
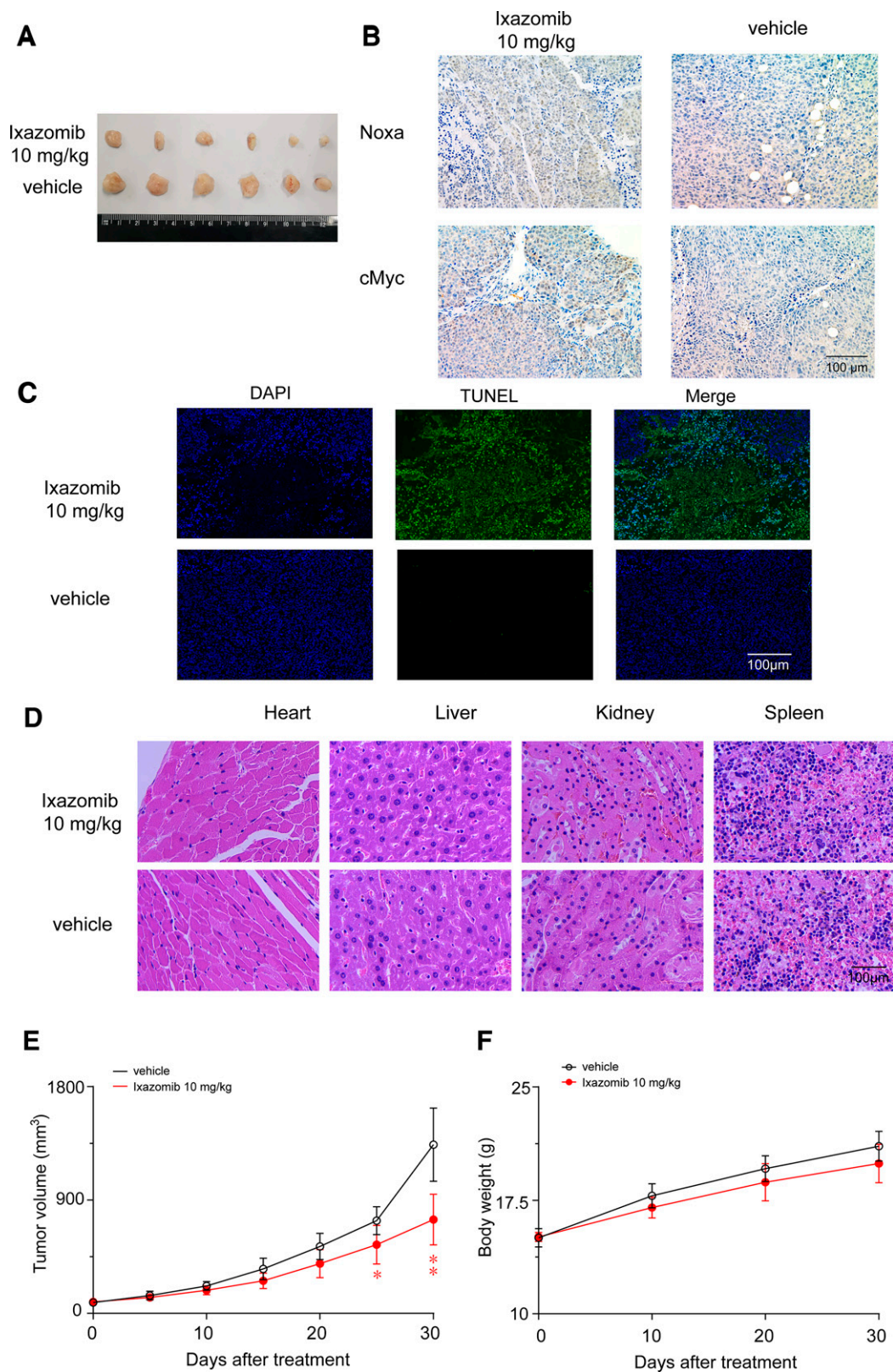
Fig. 7. Ixazomib inhibits the growth of ESCC tumors in mice xenograft models. (A) The images of xenograft tumors at the end of the experiment. (B) Representative images of NOXA and c-Myc staining of ESCC-xenografted tumor sections in different treatment groups (200× magnification). (C) The results of 4′,6-diamidino-2-phenylindole (DAPI) and TUNEL staining in different treatment groups. (D) The organs including heart, spleen, liver, and kidney from the mice treated with ixazomib 10 mg/kg were shown in the first row. The organs from the mice treated with vehicle control were shown in the second row. (E) Volume measurements of Kyse150 xenograft tumors treated with vehicle or ixazomib at the indicated dosages for 30 days. Ixazomib was administered by intragastric administration every other day at 10 mg/kg. (F) The body weight of mice in different treatment groups. Values are presented as mean ± S.D. ($n = 6$). *$P < 0.05$ or **$P < 0.01$ indicates significant differences from the vehicle group as assessed by a two-tailed unpaired Student's t test.

of overt toxicity were shown in the group (Fig. 7F). Collectively, these results suggested that ixazomib was an effective and safe antitumor drug in ESCC.

Discussion

Patients with moderate and advanced stages of ESCC lack effective systemic treatment to eradicate tumor cells, and new treatment alternatives are urgently needed to improve patient prognosis. Currently, a series of studies have supported the accumulation of ubiquitinated proteins causing tumor cell death (Soldatenkov et al., 1998; Mimnaugh et al., 2004; Itoh et al., 2019). Therefore, inducing ubiquitinated protein accumulation has become an increasingly important treatment strategy in cancer therapy, and proteasome inhibitors have been reported to have significant antitumor activity against various cancer cells through this mechanism (Sato et al., 2012; Sato et al., 2014; Sato et al., 2017). The novel oral proteasome inhibitor ixazomib is currently used for treatment of patients with multiple myeloma, and it has been confirmed to have killing efficiency to tumor cells (Sato et al., 2017; Yue and Sun, 2019; Harris et al., 2020). In this study, we explored whether the proteasome inhibitor ixazomib has therapeutic effects on ESCC. Our results proved that ixazomib effectively inhibits cell viability in ESCC cell lines and xenograft tumor model mice. Additionally, we elucidated that ixazomib induces the apoptosis and suppresses proliferation in esophageal squamous cell carcinoma through activation of the c-Myc/NOXA pathway. Moreover, our results showed that combined treatment with ixazomib and cisplatin induces synergistic anti-ESCC activity. These results clearly suggest that ixazomib has potential to be used as anti-ESCC therapeutics.

The proapoptotic NOXA is a Bcl-2 family protein, and it is a crucial role that interacts with several apoptosis-related proteins such as BCL2 associated agonist of cell death (BAD), MCL1 apoptosis regulator (MCL-1), BCL2 like 11 (BIM), and BCL2 binding component 3 (PUMA) (Morsi et al., 2018). Additionally, endoplasmic reticulum stress plays an important role in mediating tumor cell apoptosis by inducing the upregulation of NOXA (Cano-Gonzalez et al., 2018). The c-Myc oncogene is well known and acts as a driving force to activate a variety of oncogenic signaling pathways (Yoshida, 2018). c-Myc is frequently dysregulated or overexpressed in multiple tumor cells, and its abnormal expression contributes to reprogramming cell metabolism and maintaining the high rate of proliferation rate in cancer cells (Dejure and Eilers, 2017). Therefore, apoptosis in response to increased expression of c-Myc is an important endogenous protection mechanism against failure that inhibits the oncogenic properties and tumorigenesis of c-Myc (Pelengaris et al., 2002; Nilsson and Cleveland, 2003). Wirth et al. (2014) used quantitative promoter-scanning chromatin immunoprecipitation to reveal the binding of c-Myc to the promoters of NOXA upon proteasome inhibition. Other scholars also reported that c-Myc was a prime transcription factor to transactivate NOXA (Nikiforov et al., 2007). A series of studies have shown that the proteasome inhibitor bortezomib can induce c-Myc–dependent upregulation of NOXA, which leads to apoptosis in colorectal and pancreatic cancer cells (Yue and Sun, 2019; Lankes et al., 2020). Here, this study suggested that ixazomib mediated upregulation of the expression of NOXA and c-Myc in a time-dependent and concentration-dependent manner; on the other

hand, NOXA and c-Myc silencing using siRNA partially rescued the proliferation inhibitory effect of ixazomib in ESCC cells. These results confirm that ixazomib inhibits the proliferation of ESCC cells by a target on the c-Myc–NOXA pathway.

Bortezomib is the first proteasome inhibitor used as a monotherapy for the treatment of multiple myeloma and mantle cell lymphoma approved by the US Food and Drug Administration (Richardson, 2003). A series of clinical studies found that bortezomib combined with other drugs, including corticosteroids, lenalidomide, and thalidomide, can significantly improve the therapeutic effect (Kapoor et al., 2012). In recent years, research has explored the potential value of bortezomib in combination with cytotoxic drugs in solid malignancies. Bortezomib combined with platinum-based agents has achieved encouraging results in a phase I/II study in ovarian cancer and non–small-cell lung carcinomas (Ramirez et al., 2008; Piperdi et al., 2012; Zhao et al., 2015). There is a pervasive belief that the synergism between two drugs was because platinum agents can block bortezomib-induced STAT1 activation, which suppresses apoptosis (Fribley et al., 2006; Kao et al., 2013). Given that ixazomib, like bortezomib, is a boronate-based molecule, we explored whether ixazomib similarly enhances the anti-ESCC activity of the nonspecific cytotoxic agent (cisplatin and fluorouracil).

In summary, our studies have identified a novel mechanism of the proteasome inhibitor ixazomib-induced proliferation inhibition and apoptosis in ESCC. It is possible that this effect could be mediated by the c-Myc/NOXA pathway, which might give a new insight into the antitumor effect and mechanism of ixazomib in ESCC.

Authorship Contributions

Participated in research design: Wang, Zhang, Li.
Conducted experiments: Wang, Zhang, Chen, Qi, Chen, Zhu, Zhang.
Performed data analysis: Wang, Shi, Li.
Wrote or contributed to the writing of the manuscript: Wang, Zhong, Shi, Li.

References

Baou M, Kohlhaas SL, Butterworth M, Vogler M, Dinsdale D, Walewska R, Majid A, Eldering E, Dyer MJ, and Cohen GM (2010) Role of NOXA and its ubiquitination in proteasome inhibitor-induced apoptosis in chronic lymphocytic leukemia cells. *Haematologica* **95**:1510–1518.

Bard JAM, Goodall EA, Greene ER, Jonsson E, Dong KC, and Martin A (2018) Structure and Function of the 26S Proteasome. *Annu Rev Biochem* **87**:697–724.

Bray F, Ferlay J, Soerjomataram I, Siegel RL, Torre LA, and Jemal A (2018) Global cancer statistics 2018: GLOBOCAN estimates of incidence and mortality worldwide for 36 cancers in 185 countries. *CA Cancer J Clin* **68**:394–424.

Cano-González A, Mauro-Lizcano M, Iglesias-Serret D, Gil J, and López-Rivas A (2018) Involvement of both caspase-8 and Noxa-activated pathways in endoplasmic reticulum stress-induced apoptosis in triple-negative breast tumor cells. *Cell Death Dis* **9**:134.

Ciechanover A (1994) The ubiquitin-proteasome proteolytic pathway. *Cell* **79**:13–21.

Dejure FR and Eilers M (2017) MYC and tumor metabolism: chicken and egg. *EMBO J* **36**:3409–3420.

Du Y, Song L, Zhang L, Ling H, Zhang Y, Chen H, Qi H, Shi X, and Li Q (2017) The discovery of novel, potent ERR-alpha inverse agonists for the treatment of triple negative breast cancer. *Eur J Med Chem* **136**:457–467.

Ferlay J, Shin HR, Bray F, Forman D, Mathers C, and Parkin DM (2010) Estimates of worldwide burden of cancer in 2008: GLOBOCAN 2008. *Int J Cancer* **127**:2893–2917.

Fribley A, Zeng Q, and Wang CY (2004) Proteasome inhibitor PS-341 induces apoptosis through induction of endoplasmic reticulum stress-reactive oxygen species in head and neck squamous cell carcinoma cells. *Mol Cell Biol* **24**:9695–9704.

Fribley AM, Evenchik B, Zeng Q, Park BK, Guan JY, Zhang H, Hale TJ, Soengas MS, Kaufman RJ, and Wang CY (2006) Proteasome inhibitor PS-341 induces apoptosis in cisplatin-resistant squamous cell carcinoma cells by induction of Noxa. *J Biol Chem* **281**:31440–31447.

Harris MA, Miles MA, Shekhar TM, Cerra C, Georgy SR, Ryan SD, Cannon CM, and Hawkins CJ (2020) The proteasome inhibitor ixazomib inhibits the formation and growth of pulmonary and abdominal osteosarcoma metastases in mice. *Cancers (Basel)* **12**:1207.

Hochstrasser M (1995) Ubiquitin, proteasomes, and the regulation of intracellular protein degradation. *Curr Opin Cell Biol* **7**:215–223.

Hu T, Zhang J, Sha B, Li M, Wang L, Zhang Y, Liu X, Dong Z, Liu Z, Li P, et al. (2019) Targeting the overexpressed USP7 inhibits esophageal squamous cell carcinoma cell growth by inducing NOXA-mediated apoptosis. *Mol Carcinog* **58**:42–54.

Itoh A, Nonaka Y, Ogawa T, Nakamura T, and Nishi N (2019) Galectin-9 induces atypical ubiquitination leading to cell death in PC-3 prostate cancer cells. *Glycobiology* **29**:22–35.

Jana NR (2012) Protein homeostasis and aging: role of ubiquitin protein ligases. *Neurochem Int* **60**:443–447.

Johnson DE (2015) The ubiquitin-proteasome system: opportunities for therapeutic intervention in solid tumors. *Endocr Relat Cancer* **22**:T1–T17.

Kao C, Chao A, Tsai CL, Lin CY, Chuang WC, Chen HW, Yen TC, Wang TH, Lai CH, and Wang HS (2013) Phosphorylation of signal transducer and activator of transcription 1 reduces bortezomib-mediated apoptosis in cancer cells. *Cell Death Dis* **4**:e512.

Kapoor P, Ramakrishnan V, and Rajkumar SV (2012) Bortezomib combination therapy in multiple myeloma. *Semin Hematol* **49**:228–242.

Kelly KR, Espitia CM, Mahalingam D, Oyajobi BO, Coffey M, Giles FJ, Carew JS, and Nawrocki ST (2012) Reovirus therapy stimulates endoplasmic reticular stress, NOXA induction, and augments bortezomib-mediated apoptosis in multiple myeloma. *Oncogene* **31**:3023–3038.

Knorr KL, Schneider PA, Meng XW, Dai H, Smith BD, Hess AD, Karp JE, and Kaufmann SH (2015) MLN4924 induces Noxa upregulation in acute myelogenous leukemia and synergizes with Bcl-2 inhibitors. *Cell Death Differ* **22**:2133–2142.

Kupperman E, Lee EC, Cao Y, Bannerman B, Fitzgerald M, Berger A, Yu J, Yang Y, Hales P, Bruzzese F, et al. (2010) Evaluation of the proteasome inhibitor MLN9708 in preclinical models of human cancer. *Cancer Res* **70**:1970–1980.

Lankes K, Hassan Z, Doffo MJ, Schneeweis C, Lier S, Öllinger R, Rad R, Krämer OH, Keller U, Saur D, et al. (2020) Targeting the ubiquitin-proteasome system in a pancreatic cancer subtype with hyperactive MYC. *Mol Oncol* **14**:3048–3064.

Liang H, Fan JH, and Qiao YL (2017) Epidemiology, etiology, and prevention of esophageal squamous cell carcinoma in China. *Cancer Biol Med* **14**:33–41.

Lordick F, Mariette C, Haustermans K, Obermannová R, and Arnold D; ESMO Guidelines Committee (2016) Oesophageal cancer: ESMO Clinical Practice Guidelines for diagnosis, treatment and follow-up. *Ann Oncol* **27** (Suppl 5):v50–v57.

Manasanch EE and Orlowski RZ (2017) Proteasome inhibitors in cancer therapy. *Nat Rev Clin Oncol* **14**:417–433.

Mariette C, Piessen G, and Triboulet JP (2007) Therapeutic strategies in oesophageal carcinoma: role of surgery and other modalities. *Lancet Oncol* **8**:545–553.

Mimnaugh EG, Xu W, Vos M, Yuan X, Isaacs JS, Bisht KS, Gius D, and Neckers L (2004) Simultaneous inhibition of hsp 90 and the proteasome promotes protein ubiquitination, causes endoplasmic reticulum-derived cytosolic vacuolization, and enhances antitumor activity. *Mol Cancer Ther* **3**:551–566.

Minchenko OH, Tsymbal DO, Minchenko DO, and Ratushna OO (2016) The role of the TNF receptors and apoptosis inducing ligands in tumor growth. *Ukr Biochem J* **88**:18–37.

Morsi RZ, Hage-Sleiman R, Kobeissy H, and Dbaibo G (2018) Noxa: role in cancer pathogenesis and treatment. *Curr Cancer Drug Targets* **18**:914–928.

Mozos A, Roué G, López-Guillermo A, Jares P, Campo E, Colomer D, and Martinez A (2011) The expression of the endoplasmic reticulum stress sensor BiP/GRP78 predicts response to chemotherapy and determines the efficacy of proteasome inhibitors in diffuse large b-cell lymphoma. *Am J Pathol* **179**:2601–2610.

Niewerth D, Jansen G, Assaraf YG, Zweegman S, Kaspers GJ, and Cloos J (2015) Molecular basis of resistance to proteasome inhibitors in hematological malignancies. *Drug Resist Updat* **18**:18–35.

Nikiforov MA, Riblett M, Tang WH, Gratchouck V, Zhuang D, Fernandez Y, Verhaegen M, Varambally S, Chinnaiyan AM, Jakubowiak AJ, et al. (2007) Tumor cell-selective regulation of NOXA by c-MYC in response to proteasome inhibition. *Proc Natl Acad Sci USA* **104**:19488–19493.

Nilsson JA and Cleveland JL (2003) Myc pathways provoking cell suicide and cancer. *Oncogene* **22**:9007–9021.

Oakes SA and Papa FR (2015) The role of endoplasmic reticulum stress in human pathology. *Annu Rev Pathol* **10**:173–194.

Ooko E, Kadioglu O, Greten HJ, and Efferth T (2017) Pharmacogenomic characterization and isobologram analysis of the combination of ascorbic acid and curcumin-two main metabolites of *Curcuma longa*-in cancer cells. *Front Pharmacol* **8**:38.

Pelengaris S, Khan M, and Evan G (2002) c-MYC: more than just a matter of life and death. *Nat Rev Cancer* **2**:764–776.

Piperdi B, Walsh WV, Bradley K, Zhou Z, Bathini V, Hanrahan-Boshes M, Hutchinson L and Perez-Soler R (2012) Phase-I/II study of bortezomib in combination with carboplatin and bevacizumab as first-line therapy in patients with advanced non-small-cell lung cancer. *J Thorac Oncol* **7**:1032–1040.

Ramirez PT, Landen Jr CN, Coleman RL, Milam MR, Levenback C, Johnston TA, and Gershenson DM (2008) Phase I trial of the proteasome inhibitor bortezomib in combination with platinum- and taxane-resistant ovarian cancer. *Gynecol Oncol* **108**:68–71.

Richardson P (2003) Clinical update: proteasome inhibitors in hematologic malignancies. *Cancer Treat Rev* **29** (Suppl 1):33–39.

Rosekrans SL, Heijmans J, Büller NV, Westerlund J, Lee AS, Muncan V, and van den Brink GR (2015) ER stress induces epithelial differentiation in the mouse oesophagus. *Gut* **64**:195–202.

Sato A, Asano T, Ito K, and Asano T (2012) Vorinostat and bortezomib synergistically cause ubiquitinated protein accumulation in prostate cancer cells. *J Urol* **188**:2410–2418.

Sato A, Asano T, Isono M, Ito K, and Asano T (2014) Panobinostat synergizes with bortezomib to induce endoplasmic reticulum stress and ubiquitinated protein accumulation in renal cancer cells. *BMC Urol* **14**:71.

Sato A, Asano T, Okubo K, Isono M, and Asano T (2017) Ritonavir and ixazomib kill bladder cancer cells by causing ubiquitinated protein accumulation. *Cancer Sci* **108**:1194–1202.

Shirley M (2016) Ixazomib: first global approval. *Drugs* **76**:405–411.

Soldatenkov VA, Prasad S, Voloshin Y, and Dritschilo A (1998) Sodium butyrate induces apoptosis and accumulation of ubiquitinated proteins in human breast carcinoma cells. *Cell Death Differ* **5**:307–312.

Sosa Seda IM, Mott JL, Akazawa Y, Barreyro FJ, Bronk SF, Kaufmann SH, and Gores GJ (2010) Noxa mediates hepatic stellate cell apoptosis by proteasome inhibition. *Hepatology Res* **40**:701–710.

Wirth M, Stojanovic N, Christian J, Paul MC, Stauber RH, Schmid RM, Häcker G, Krämer OH, Saur D, and Schneider G (2014) MYC and EGR1 synergize to trigger tumor cell death by controlling NOXA and BIM transcription upon treatment with the proteasome inhibitor bortezomib. *Nucleic Acids Res* **42**:10433–10447.

Yoshida GJ (2018) Emerging roles of Myc in stem cell biology and novel tumor therapies. *J Experimental Clin Cancer Res* **37**:173.

Yue D and Sun X (2019) Ixazomib promotes CHOP-dependent DR5 induction and apoptosis in colorectal cancer cells. *Cancer Biol Ther* **20**:284–294.

Zhang L, Liu P, Chen H, Li Q, Chen L, Qi H, Shi X, and Du Y (2016) Characterization of a selective inverse agonist for estrogen related receptor α as a potential agent for breast cancer. *Eur J Pharmacol* **789**:439–448.

Zhang L, Zhu Y, Cheng H, Zhang J, Zhu Y, Chen H, Chen L, Qi H, Ren G, Tang J, et al. (2019) The increased expression of estrogen-related receptor α correlates with Wnt5a and poor prognosis in patients with glioma. *Mol Cancer Ther* **18**:173–184.

Zhao J, He YT, Zheng RS, Zhang SW, and Chen WQ (2012) Analysis of esophageal cancer time trends in China, 1989-2008. *Asian Pac J Cancer Prev* **13**:4613–4617.

Zhao Y, Foster NR, Meyers JP, Thomas SP, Northfelt DW, Rowland KM Jr, Mattar BI, Johnson DB, Molina JR, Mandrekar SJ, Schild SE, Bearden JD III, Aubry MC and Adjei AA (2015) A phase I/II study of bortezomib in combination with paclitaxel, carboplatin, and concurrent thoracic radiation therapy for non-small-cell lung cancer: North Central Cancer Treatment Group (NCCTG-N0321. *J Thoracic Oncol* **10**:172–180.

Address correspondence to: Qunyi Li, Department of Pharmacy, Huashan Hospital, Fudan University, No.12 Urumqi Middle Rd., Shanghai 200040, China. E-mail: qyli1234@163.com; or Xiaojin Shi, Department of Pharmacy, Huashan Hospital, Fudan University, No.12 Urumqi Middle Rd., Shanghai 200040, China. E-mail: xiaojin_shi@hotmail.com